Conf-781128--11

A POWER AND PHASE MONITORING SYSTEM FOR THE LOWER HYBRID PHASED ARRAY HEATING SYSTEM ON ATC MACHINE

Brent W. Reed
Princeton University, Plasma Physics Laboratory
Princeton, New Jersey 08540

Summary

A four waveguide phased array slow wave structure has been constructed to couple microwave energy into plasma in the ATC Tokamac at Princeton. Theory has indicated that the coupling of power into the plasma column is a strong function of the imposed fourier spectrum at the antenna aperture.[1]

To optimize heating, and to verify theoretical results, a precision amplitude and phase monitoring system has been designed and constructed. The system data output is routed to an IBM 1800 computer where the fourier spectrum in $n_{||}$ space is computed for discrete increments of time during an RF pulse. Computer output data is used to update the adjustment of transmission line parameters inbetween pulses.

The RF power source consists of four independent 50 kW klystrons driven from a common exciter with phase shifters and attenuators utilized in the low level drive circuits to control the klystron outputs. 50Ω, 3-1/8 inch coax lines are run to the ATC platform where transitions are made to WR-975 waveguide. Triple-stub waveguide tuners are also provided in the transmission loop to aid matching.

The system contains 8 bi-directional couplers, one before and one after the tuner in each line. Square law back diode detectors provide gross power in and power out measurements at each directional coupler while quadrature detectors after the tuners are used to measure amplitude and phase of the forward and reverse voltage waves.

Homodyne quadrature detectors are constructed from double balanced mixers and 90° hybrids. A sample of the exciter signal is split and fed in phase to each mixer thus providing a fixed reference phase for all measurements.

A waveguide system is calibrated before installation and all relative phase lengths from the directional couplers are measured to a common reference flange with dowel pins insuring proper mechanical alignment. A short at the reference flange establishes a reflection coefficient of $\rho = -1$ for each line.

Correction constants are stored in a computer system so that data is automatically scaled. A test [illegible] for each RF pulse which permits

System

The end product of the monitoring system graphic computer output of forward and reverse power versus time for each waveguide in an array (Fig. 1), and a series of plots of the spectrum of the radiation fields in front of array in $n_{||}$ space (parallel to the toroidal magnetic field on ATC). This output is used assist system tuning (an involved process of acting adjustments) and to evaluate theory.

Although directional couplers, tuners and detection equipment are located on the ATC p to minimize errors due to carrier frequency temperature and load changes, a grounding pr is created because of the stray ohmic heatin in the vicinity. Considerable caution is ta eliminate ground loops which would disturb m ments. All detection electronics are enclos an RFI shielded rack into which enters only nals and 60 cycle power. Outputs are differ driven shielded twisted pairs.

RF System Outputs

Quantity	Description
4	Before tuner forward
4	Before tuner reverse
4	After tuner forward
4	After tuner reverse
16	After tuner quadratu components
Total 32	

The Data Aquisition Services group at built a 32 channel analog magnetic drum tr recording system (Fig. 2) with a 100 KHz ba and a 50 ms track length. Its differential are driven directly by the monitoring syst Since the drum is several hundred feet fro machine platform, the twisted pairs are pr terminated on both ends. The analog signa FM modulated before recording. When read they are demodulated, filtered and digitiz software selectable but maximum rate of 1 every 10 μs. One 20 ms experiment generat 10 bit words when digitized at maximum thr The interface to the DAS-1800 computer (al designed and constructed by DAS) cannot pa process this much data in-between events (apart) so a PDP-8/I, designated to the co

Conf-781125-116

A POWER AND PHASE MONITORING SYSTEM FOR THE LOWER HYBRID PHASED ARRAY HEATING SYSTEM ON ATC MACHINE

Brent W. Reed
Princeton University, Plasma Physics Laboratory
Princeton, New Jersey 08540

System

The end product of the monitoring system is graphic computer output of forward and reverse power versus time for each waveguide in an antenna array (Fig. 1), and a series of plots of the fourier spectrum of the radiation fields in front of the array in $n_{||}$ space (parallel to the toroidal magnetic field on ATC). This output is used to assist system tuning (an involved process of interacting adjustments) and to evaluate theory.

Although directional couplers, tuners and detection equipment are located on the ATC platform to minimize errors due to carrier frequency drift, temperature and load changes, a grounding problem is created because of the stray ohmic heating fields in the vicinity. Considerable caution is taken to eliminate ground loops which would disturb measurements. All detection electronics are enclosed in an RFI shielded rack into which enters only RF signals and 60 cycle power. Outputs are differentially driven shielded twisted pairs.

RF System Outputs

Quantity	Description
4	Before tuner forward power
4	Before tuner reverse power
4	After tuner forward power
4	After tuner reverse power
16	After tuner quadrature components
Total 32	

The Data Aquisition Services group at PPL has built a 32 channel analog magnetic drum transient recording system (Fig. 2) with a 100 KHz bandwidth and a 50 ms track length. Its differential inputs are driven directly by the monitoring system outputs. Since the drum is several hundred feet from the machine platform, the twisted pairs are properly terminated on both ends. The analog signals are FM modulated before recording. When read back, they are demodulated, filtered and digitized at a software selectable but maximum rate of 1 point every 10 μs. One 20 ms experiment generates 64K 10 bit words when digitized at maximum throughput. The interface to the DAS-1800 computer (also designed and constructed by DAS) cannot pass and process this much data in-between events (90 sec. apart) so a PDP-8/I, designated to the control of data transfer, is used to block out a much smaller,

A four waveguide phased array slow wave structure has been constructed to couple microwave energy into plasma in the ATC Tokamac at Princeton. Theory has indicated that the coupling of power into the plasma column is a strong function of the imposed fourier spectrum at the antenna aperture.[1]

To optimize heating, and to verify theoretical results, a precision amplitude and phase monitoring system has been designed and constructed. The system data output is routed to an IBM 1800 computer where the fourier spectrum in $n_{||}$ space is computed for discrete increments of time during an RF pulse. Computer output data is used to update the adjustment of transmission line parameters inbetween pulses.

The RF power source consists of four independent 50 kW klystrons driven from a common exciter with phase shifters and attenuators utilized in the low level drive circuits to control the klystron outputs. 50Ω, 3-1/8 inch coax lines are run to the ATC platform where transitions are made to WR-975 waveguide. Triple-stub waveguide tuners are also provided in the transmission loop to aid matching.

The system contains 8 bi-directional couplers, one before and one after the tuner in each line. Square law back diode detectors provide gross power in and power out measurements at each directional coupler while quadrature detectors after the tuners are used to measure amplitude and phase of the forward and reverse voltage waves.

Homodyne quadrature detectors are constructed from double balanced mixers and 90° hybrids. A sample of the exciter signal is split and fed in phase to each mixer thus providing a fixed reference phase for all measurements.

A waveguide system is calibrated before installation and all relative phase lengths from the directional couplers are measured to a common reference flange with dowel pins insuring proper mechanical alignment. A short at the reference flange establishes a reflection coefficient of $\rho = -1$ for each line.

Correction constants are stored in a computer system so that data is automatically scaled. A test signal is applied before each RF pulse which permits computation of the gain and offset of each data channel.

Data is stored in real time on a 32 channel analog magnetic drum recorder. A PDP-8/I is used as a data controller-buffer to transfer information from the A/D converter on the drum output into the IBM 1800 where processing takes place.

Interactive program control permits a choice of observation time and displayed data via a CRT graphic terminal.

The end product of the monitoring syst graphic computer output of forward and reve power versus time for each waveguide in an array (Fig. 1), and a series of plots of th spectrum of the radiation fields in front o array in $n_{||}$ space (parallel to the toroi magnetic field on ATC). This output is use assist system tuning (an involved process o acting adjustments) and to evaluate theory.

Although directional couplers, tuners detection equipment are located on the ATC to minimize errors due to carrier frequency temperature and load changes, a grounding p is created because of the stray ohmic heati in the vicinity. Considerable caution is t eliminate ground loops which would disturb ments. All detection electronics are enclos an RFI shielded rack into which enters only nals and 60 cycle power. Outputs are diffe driven shielded twisted pairs.

RF System Outputs

Quantity	Description
4	Before tuner forward
4	Before tuner reverse
4	After tuner forward
4	After tuner reverse
16	After tuner quadratur components
Total 32	

The Data Aquisition Services group at built a 32 channel analog magnetic drum tra recording system (Fig. 2) with a 100 KHz ba and a 50 ms track length. Its differential are driven directly by the monitoring syste Since the drum is several hundred feet from machine platform, the twisted pairs are pro terminated on both ends. The analog signal FM modulated before recording. When read b they are demodulated, filtered and digitize software selectable but maximum rate of 1 p every 10 μs. One 20 ms experiment generate 10 bit words when digitized at maximum thro The interface to the DAS-1800 computer (als designed and constructed by DAS) cannot pas process this much data in-between events (9 apart) so a PDP-8/I, designated to the cont data transfer, is used to block out a each software selectable, segment of data over a time span for transfer to the DAS-180C.

A calibration pulse, generated on the and applied to each signal input, is freshly ed on the drum each cycle and is used to co gain and offset drift errors during analysis

Since the drum is a relatively noisy s (50 mV rms noise at 100 KHz BW), a programmat

The end product of the monitoring system is graphic computer output of forward and reverse power versus time for each waveguide in an antenna array (Fig. 1), and a series of plots of the fourier spectrum of the radiation fields in front of the array in $n_{\parallel}$ space (parallel to the toroidal magnetic field on ATC). This output is used to assist system tuning (an involved process of interacting adjustments) and to evaluate theory.

Although directional couplers, tuners and detection equipment are located on the ATC platform to minimize errors due to carrier frequency drift, temperature and load changes, a grounding problem is created because of the stray ohmic heating fields in the vicinity. Considerable caution is taken to eliminate ground loops which would disturb measurements. All detection electronics are enclosed in an RFI shielded rack into which enters only RF signals and 60 cycle power. Outputs are differentially driven shielded twisted pairs.

RF System Outputs

Quantity	Description
4	Before tuner forward power
4	Before tuner reverse power
4	After tuner forward power
4	After tuner reverse power
16	After tuner quadrature components
Total 32	

The Data Aquisition Services group at PPL has built a 32 channel analog magnetic drum transient recording system (Fig. 2) with a 100 KHz bandwidth and a 50 ms track length. Its differential inputs are driven directly by the monitoring system outputs. Since the drum is several hundred feet from the machine platform, the twisted pairs are properly terminated on both ends. The analog signals are FM modulated before recording. When read back, they are demodulated, filtered and digitized at a software selectable but maximum rate of 1 point every 10 us. One 20 ms experiment generates 64K 10 bit words when digitized at maximum throughput. The interface to the DAS-1800 computer (also designed and constructed by DAS) cannot pass and process this much data in-between events (90 sec. apart) so a PDP-8/I, designated to the control of data transfer, is used to block out a much smaller, software selectable, segment of data over a limited time span for transfer to the DAS-1800.

A calibration pulse, generated on the platform and applied to each signal input, is freshly recorded on the drum each cycle and is used to correct gain and offset drift errors during analysis.

Since the drum is a relatively noisy system (50 mV rms noise at 100 KHz BW), a programmable

gain amplifier is included after each detector output to improve the dynamic range of the system to the limit imposed by the noise of the first amplifier. The bi-polar drum inputs may swing ±4 volts before saturation for an inherent maximum signal to noise ratio of 40 dB over the 100 KHz maximum bandwidth. An active filter may be placed in the drum output circuitry, limiting the bandwidth to a few KHz, but improving the maximum S/N ratio to 52 dB when maximum bandwidth is not required. The noise contribution of the amplifiers immediately following the detectors is about 5 mV rms over a 100 KHz bandwidth. Full bandwidth system dynamic range for a 10 dB S/N ratio is, therefore, about 48 dB (61 with filtering). The dynamic range of a square law input is the same as cited above. However, a linear detector has double the input dynamic range of the square law type.

Transmission System

The transmission system is comprised of four identical paths as shown in Fig. 3. The first tuner is a low VSWR tuner which is used to match the source to the waveguide, thus eliminating mismatch errors due to multiple reflections between source and load. The source is matched when variation occuring in the directional coupler output levels is minimized.

Since the directivity of the couplers is about 33 dB and the coupling coefficient is known to ±0.06 dB, the minimum uncertainty of about ±0.25 dB exists in the coupler before the second tuner. The couplers are of the below cut-off loop type, and since their directivity is critically affected by the output load impedance, well matched pads are used to isolate all detectors and transmission lines from the coupler outputs.

Tuner 2 is a high VSWR tuner which is used to optimize power transfer to the plasma. The fourier spectrum is constructed from the data taken from the second set of couplers, while the first set is used to absolute power measurements. Although square law detectors are provided after tuner 2, they are only used to double check the computerized analysis.

The Square Law Detector

The power detectors are designed to operate in the square law region using back diodes rather than conventional point contact or Schottky types. The back diode[2] is a tunnel diode which is doped to minimize the peak in the forward V-I characteristic. It has two main advantages[3] in this application:

(1) A very low reverse threshold voltage.

(2) Less than 30% of the sensitivity of vol-

Three mechanisms in the detector c produce thermal drift:

(1) Thermocouple effects.

(2) Component value drifts.

(3) Diode V-I characteristic chan

Although little can be done to minimize couple effects, the following measures to minimize the other drift effects:

(1) NPO capacitors are used to ma stability.

(2) Capacitors are mounted with m length to minimize exaggerate changes due to lead resonance

(3) A negative temperature coeffi thermister is used for a dete in order to cancel changes in

Although the load resistor affects quency response of the detector, the ch negligible because of the band limiting istics of subsequent stages.

Figure 8 shows the video bandwidth detector itself, which is constructed i form on a double-sided circuit board usi 2 oz.,1/16" material. The video bandwi greatly increased for other application ing the capacitor values.

An operational amplifier using an follows the detector, operating with a gain of about 50. Offset correction is and low thermal drift gain setting comp used. Figure 8 also shows a plot of it loop frequency and phase response. The expected RF input will cause a 4V output stage.

The detector and amplifier which a same circuit board are enclosed in a st suppress magnetically induced transient

The Phase Detector Design

A simple, reliable, inexpensive ph tor[4,5] design is required which utilize obtained stock components. Since the R source for the entire heating system i a homodyne detection scheme is chosen u double-balanced, broadband mixer.

A double balanced mixer (Figure 6 structed in such a way as to produce c isolation between ports. When the RF are 90° out of phase, there is no IF o

Three mechanisms in the detector circuit produce thermal drift:

(1) Thermocouple effects.

(2) Component value drifts.

(3) Diode V-I characteristic changes.

Although little can be done to minimize thermocouple effects, the following measures are taken to minimize the other drift effects:

(1) NPO capacitors are used to maximum stability.

(2) Capacitors are mounted with minimum lead length to minimize exaggerated reactance changes due to lead resonances.

(3) A negative temperature coefficient thermister is used for a detector load in order to cancel changes in the diodes.

Although the load resistor affects the frequency response of the detector, the change is negligible because of the band limiting characteristics of subsequent stages.

Figure 8 shows the video bandwidth of the detector itself, which is constructed in discrete form on a double-sided circuit board using G-10 2 oz., 1/16" material. The video bandwidth may be greatly increased for other applications by reducing the capacitor values.

An operational amplifier using an LH0062CH follows the detector, operating with a voltage gain of about 50. Offset correction is provided, and low thermal drift gain setting components are used. Figure 8 also shows a plot of its closed loop frequency and phase response. The maximum expected RF input will cause a 4V output from the stage.

The detector and amplifier which are on the same circuit board are enclosed in a steel box to suppress magnetically induced transients.

The Phase Detector Design

A simple, reliable, inexpensive phase detector[4,5] design is required which utilizes easily obtained stock components. Since the RF drive source for the entire heating system is available, a homodyne detection scheme is chosen utilizing a double-balanced, broadband mixer.

A double balanced mixer (Figure 6) is constructed in such a way as to produce considerable isolation between ports. When the RF and LO inputs are 90° out of phase, there is no IF output. When in phase a positive difference product is seen at the IF output, and when the inputs are 180° out of phase, a negative IF difference output is generated.

noise contribution of the amplifiers immediately following the detectors is about 5 mV rms over a 100 KHz bandwidth. Full bandwidth system dynamic range for a 10 dB S/N ratio is, therefore, about 48 dB (61 with filtering). The dynamic range of a square law input is the same as cited above. However, a linear detector has double the input dynamic range of the square law type.

Transmission System

The transmission system is comprised of four identical paths as shown in Fig. 3. The first tuner is a low VSWR tuner which is used to match the source to the waveguide, thus eliminating mismatch errors due to multiple reflections between source and load. The source is matched when variation occuring in the directional coupler output levels is minimized.

Since the directivity of the couplers is about 33 dB and the coupling coefficient is known to ±0.06 dB, the minimum uncertainty of about ±0.25 dB exists in the coupler before the second tuner. The couplers are of the below cut-off loop type, and since their directivity is critically affected by the output load impedance, well matched pads are used to isolate all detectors and transmission lines from the coupler outputs.

Tuner 2 is a high VSWR tuner which is used to optimize power transfer to the plasma. The fourier spectrum is constructed from the data taken from the second set of couplers, while the first set is used to absolute power measurements. Although square law detectors are provided after tuner 2, they are only used to double check the computerized analysis.

The Square Law Detector

The power detectors are designed to operate in the square law region using back diodes rather than conventional point contact or Schottky types. The back diode[2] is a tunnel diode which is doped to minimize the peak in the forward V-I characteristic. It has two main advantages[3] in this application:

(1) A very low reverse threshold voltage.

(2) Less than 30% of the sensitivity of voltage drop at fixed current than manifested by point contact and Schottky types which manifest about 0.3%°C change.

Figure 4 shows the V-I curve of the GE BD-3 back diode chosen for the voltage doubling detector (Figure 5) used in this application. The voltage doubling detector is used to minimize the required amplification after the detector. Figure 7 shows the typical detector output vs. the RF input.

to minimize the other drift effects:

(1) NPO capacitors are used to maximu stability.

(2) Capacitors are mounted with minim length to minimize exaggerated re changes due to lead resonances.

(3) A negative temperature coefficien thermister is used for a detecto in order to cancel changes in the

Although the load resistor affects the quency response of the detector, the change negligible because of the band limiting cha istics of subsequent stages.

Figure 8 shows the video bandwidth of detector itself, which is constructed in di form on a double-sided circuit board using 2 oz.,1/16" material. The video bandwidth greatly increased for other applications by ing the capacitor values.

An operational amplifier using an LH0 follows the detector, operating with a volt gain of about 50. Offset correction is pro and low thermal drift gain setting compone used. Figure 9 also shows a plot of its cl loop frequency and phase response. The max expected RF input will cause a 4V output fr stage.

The detector and amplifier which are same circuit board are enclosed in a steel suppress magnetically induced transients.

The Phase Detector Design

A simple, reliable, inexpensive phase tor[4,5] design is required which utilizes obtained stock components. Since the RF d source for the entire heating system is av a homodyne detection scheme is chosen util double-balanced, broadband mixer.

A double balanced mixer (Figure 6) s structed in such a way as to produce consi isolation between ports. When the RF and are 90° out of phase, there is no IF outpu in phase a positive difference product is the IF output, and when the inputs are 180 phase, a negative IF difference output is

If the RF port input level is at leas lower than the LO drive level, such a mix extremely linear: the greater differential levels, the greater the linearity. As the and LO drive approach the same level, the becomes very non-linear. The excellent li

(1) NPO capacitors are used to [illegible] stability.

(2) Capacitors are mounted with minimum lead length to minimize exaggerated reactance changes due to lead resonances.

(3) A negative temperature coefficient thermister is used for a detector load in order to cancel changes in the diodes.

Although the load resistor affects the frequency response of the detector, the change is negligible because of the band limiting characteristics of subsequent stages.

Figure 8 shows the video bandwidth of the detector itself, which is constructed in discrete form on a double-sided circuit board using G-10 2 oz.,1/16" material. The video bandwidth may be greatly increased for other applications by reducing the capacitor values.

An operational amplifier using an LH0062CH follows the detector, operating with a voltage gain of about 50. Offset correction is provided, and low thermal drift gain setting components are used. Figure 8 also shows a plot of its closed loop frequency and phase response. The maximum expected RF input will cause a 4V output from the stage.

The detector and amplifier which are on the same circuit board are enclosed in a steel box to suppress magnetically induced transients.

The Phase Detector Design

A simple, reliable, inexpensive phase detector[4,5] design is required which utilizes easily obtained stock components. Since the RF drive source for the entire heating system is available, a homodyne detection scheme is chosen utilizing a double-balanced, broadband mixer.

A double balanced mixer (Figure 6) is constructed in such a way as to produce considerable isolation between ports. When the RF and LO inputs are 90° out of phase, there is no IF output. When in phase a positive difference product is seen at the IF output, and when the inputs are 180° out of phase, a negative IF difference output is generated.

If the RF port input level is at least 10 dB lower than the LO drive level, such a mixer is extremely linear: the greater differential in drive levels, the greater the linearity. As the RF drive and LO drive approach the same level, the mixer becomes very non-linear. The excellent linearity

4

arises from the fact that the diodes are turned on by the LO while the RF drive produces only an infinitesimal excursion on the diode V-I curve.

The double balanced mixer is a natural choice for a high linearity, phase sensitive detector. Furthermore, it is an inexpensive, stock item from many manufacturers.

Mixer diode inbalance may produce some slight dc offset at the IF output with only LO drive present. This offset is somewhat stable with temperature because the diodes, although not stable themselves, track quite well with temperature. The offset correction process described in the calibration section minimizes this source of error. Conversion loss changes with temperature for the mixers are considered negligible. The primary causes of mixer temperature sensitivity are ferrite losses in the mixer baluns and transformers.

A quadrature detector system (Figure 9), similar to that used in color television receivers, is used to resolve an RF input voltage vector into a cartesian coordinate system. A stripline $\pi/2$ hybrid splits the RF input into two signals 90° out of phase. The mixers are used to obtain the difference beats, which are dc coupled baseband signals. The low pass filters which follow, remove the unwanted fundamental and mixer products eliminating RF interference to the instrumentation amplifiers.

The instrumentation amplifier is of the same design used for the square law detector with the same board layout and the same steel enclosure being utilized, thus simplifying hardware requirements.

Since the transient recorder inputs are bipolar, the mixer outputs are not offset.

0 to 90° phase shifters are provided before each mixer LO input which are used to trim out stray phase shifts in the system in order to bring the mixers into perfect quadrature operation. Gain controls on the amplifiers compensate for small differences in RF and mixer conversion losses.

The exciter sample, used to drive the local oscillator inputs to the quadrature detector assemblies is taken from a 20 dB directional coupler from the exciter output (Figure 10). A long RG-8A/U coax run brings the signal to the machine platform which is then amplified and split in phase 16 ways for the mixers. Additional high level isolated, well matched output ports are provided for system testing. A maximum of 1 watt is available which is the maximum level ever expected at a waveguide directional coupler output port.

The two single stage, medium power amplifiers used in the system test output section are designed by PPL. The first stage is a class A unit while

Calibration Procedures

The input offset drift of the fi
is typically 10μv/°C, and the drift c
from the programmable gain stages dif
drivers, receivers and the drum recor
ics is substantially larger. It ther
necessary to correct offset errors.
thermal drift first stage gain is con
negligible, the gain variation of the
stages is not.

The drum recording is started 10
RF is turned on. During this interva
offset errors are recognized as the i
After 5 ms, a calibration signal is u
the first gain stage thus eliminating
disturb sensitive input circuitry, an
very low calibration voltages accurat

The magnitude of the calibration
is accurately known and is a function
setting of the programmable gain stag
set data is used to correct the test
while neglecting the relatively small
tribution of the first stage, which i
turn used to correct the actual data
by the DAS-1800.

Analog signal outputs are availab
drum so that signals may be viewed on
pictures taken, and data analyzed by h
computer results. Since the calibrati
is also displayed, corrections may al
by hand.

Special consideration is also gi
guide calibrations. Knowledge of the
trical length from the directional co
to the array apertures is obtained in
(1) The electrical lengths of each f
pared to one chosen as a reference.
ments are made by transmission. (2)
placed on the reference flange (Figur
joint between the feed and the array
angle between the forward and reverse
defined by that short. All measureme
fore made with respect to the referen
Smith chart type analysis must be don
find the relationships between forwar
wave components in the apertures the

All of the phase constants are a
measured with a precision constant in
stretcher and vector voltmeter.

Data Processing

The fourier spectrum discussed e
result of an integration[6]:

$$f(k) = \frac{1}{\sqrt{2\pi}} \int_{-\infty}^{\infty} f(x)\, e^{jkx} dx \quad \text{wh}$$

Calibration Procedures

The input offset drift of the first gain stage is typically 10μv/°C, and the drift contribution from the programmable gain stages differential drivers, receivers and the drum recording electronics is substantially larger. It therefore is necessary to correct offset errors. Although thermal drift first stage gain is considered negligible, the gain variation of the following stages is not.

The drum recording is started 10 ms before the RF is turned on. During this interval, the total offset errors are recognized as the input voltages. After 5 ms, a calibration signal is used to replace the first gain stage thus eliminating the need to disturb sensitive input circuitry, and maintain very low calibration voltages accurately.

The magnitude of the calibration signal voltage is accurately known and is a function of the gain setting of the programmable gain stages. The offset data is used to correct the test signal data while neglecting the relatively small offset contribution of the first stage, which is then in turn used to correct the actual data set stored by the DAS-1800.

Analog signal outputs are available from the drum so that signals may be viewed on oscilloscopes, pictures taken, and data analyzed by hand to check computer results. Since the calibration interval is also displayed, corrections may also be made by hand.

Special consideration is also given to waveguide calibrations. Knowledge of the exact electrical length from the directional coupler ports to the array apertures is obtained in two steps: (1) The electrical lengths of each feed are compared to one chosen as a reference. These measurements are made by transmission. (2) A short is placed on the reference flange (Figure 1) at the joint between the feed and the array structure, the angle between the forward and reverse waves being defined by that short. All measurements are therefore made with respect to the reference flange. Smith chart type analysis must be done in order to find the relationships between forward and reverse wave components in the apertures themselves.

All of the phase constants are accurately measured with a precision constant impedance line stretcher and vector voltmeter.

Data Processing

The fourier spectrum discussed earlier is the result of an integration[6]:

$$f(k) = \frac{1}{\sqrt{2\pi}} \int_{-\infty}^{\infty} f(x)\, e^{jkx} dx \quad \text{where}$$

$$f(x) = A_1 e^{\frac{p}{2}} \quad -2L < x < -L$$

present. This offset is somewhat stable with temperature because the diodes, although not stable themselves, track quite well with temperature. The offset correction process described in the calibration section minimizes this source of error. Conversion loss changes with temperature for the mixers are considered negligible. The primary causes of mixer temperature sensitivity are ferrite losses in the mixer baluns and transformers.

A quadrature detector system (Figure 9), similar to that used in color television receivers, is used to resolve an RF input voltage vector into a cartesian coordinate system. A stripline $\pi/2$ hybrid splits the RF input into two signals 90° out of phase. The mixers are used to obtain the difference beats, which are dc coupled baseband signals. The low pass filters which follow, remove the unwanted fundamental and mixer products eliminating RF interference to the instrumentation amplifiers.

The instrumentation amplifier is of the same design used for the square law detector with the same board layout and the same steel enclosure being utilized, thus simplifying hardware requirements.

Since the transient recorder inputs are bipolar, the mixer outputs are not offset.

0 to 90° phase shifters are provided before each mixer LO input which are used to trim out stray phase shifts in the system in order to bring the mixers into perfect quadrature operation. Gain controls on the amplifiers compensate for small differences in RF and mixer conversion losses.

The exciter sample, used to drive the local oscillator inputs to the quadrature detector assemblies is taken from a 20 dB directional coupler from the exciter output (Figure 10). A long RG-8A/U coax run brings the signal to the machine platform which is then amplified and split in phase 16 ways for the mixers. Additional high level isolated, well matched output ports are provided for system testing. A maximum of 1 watt is available which is the maximum level ever expected at a waveguide directional coupler output port.

The two single stage, medium power amplifiers used in the system test output section are designed by PPL. The first stage is a class A unit while the second stage is class C. Although the cascade is capable of delivering over 5 watts, the output is limited to about a watt to protect the attenuators. If the attenuators are placed at the input to the chain, very non-linear output changes are produced because of being very close to the drive threshold for class C operation of the final stage. The transistor chosen for the final stage must be used in a common base configuration, and class B biasing would require an additional power supply, an expense eliminated by the circuit configuration which has been chosen.

The drum recording is started 10 ms be RF is turned on. During this interval, the t offset errors are recognized as the input vo After 5 ms, a calibration signal is used to the first gain stage thus eliminating the ne disturb sensitive input circuitry, and maint very low calibration voltages accurately.

The magnitude of the calibration signal is accurately known and is a function of the setting of the programmable gain stages. Th set data is used to correct the test signal while neglecting the relatively small offset tribution of the first stage, which is then turn used to correct the actual data set sto by the DAS-1800.

Analog signal outputs are available fro drum so that signals may be viewed on oscill pictures taken, and data analyzed by hand to computer results. Since the calibration int is also displayed, corrections may also be by hand.

Special consideration is also given to guide calibrations. Knowledge of the exact trical length from the directional coupler p to the array apertures is obtained in two st (1) The electrical lengths of each feed are pared to one chosen as a reference. These ments are made by transmission. (2) A shor placed on the reference flange (Figure 1) a joint between the feed and the array structu angle between the forward and reverse waves defined by that short. All measurements ar fore made with respect to the reference fla Smith chart type analysis must be done in o find the relationships between forward and wave components in the apertures themselves.

All of the phase constants are accurat measured with a precision constant impedanc stretcher and vector voltmeter.

Data Processing

The fourier spectrum discussed earlier result of an integration[6]:

$$f(k) = \frac{1}{\sqrt{2\pi}} \int_{-\infty}^{\infty} f(x)\, e^{jkx} dx \quad \text{where}$$

$$f(x) = A_1 e^{j\phi_1} \quad -2L < x < -L$$

$$= A_2 e^{j\phi_2} \quad -L < x < 0$$

$$= A_3 e^{j\phi_3} \quad 0 < x < L$$

$$= A_4 e^{j\phi_4} \quad L < x < 2L$$

The drum recording is started 10 [illegible] before the RF is turned on. During this interval, the total offset errors are recognized as the input voltages. After 5 ms, a calibration signal is used to replace the first gain stage thus eliminating the need to disturb sensitive input circuitry, and maintain very low calibration voltages accurately.

The magnitude of the calibration signal voltage is accurately known and is a function of the gain setting of the programmable gain stages. The offset data is used to correct the test signal data while neglecting the relatively small offset contribution of the first stage, which is then in turn used to correct the actual data set stored by the DAS-1800.

Analog signal outputs are available from the drum so that signals may be viewed on oscilloscopes, pictures taken, and data analyzed by hand to check computer results. Since the calibration interval is also displayed, corrections may also be made by hand.

Special consideration is also given to waveguide calibrations. Knowledge of the exact electrical length from the directional coupler ports to the array apertures is obtained in two steps: (1) The electrical lengths of each feed are compared to one chosen as a reference. These measurements are made by transmission. (2) A short is placed on the reference flange (Figure 1) at the joint between the feed and the array structure, the angle between the forward and reverse waves being defined by that short. All measurements are therefore made with respect to the reference flange. Smith chart type analysis must be done in order to find the relationships between forward and reverse wave components in the apertures themselves.

All of the phase constants are accurately measured with a precision constant impedance line stretcher and vector voltmeter.

Data Processing

The fourier spectrum discussed earlier is the result of an integration[6]:

$$f(k) = \frac{1}{\sqrt{2\pi}} \int_{-\infty}^{\infty} f(x)\, e^{jkx} dx \quad \text{where}$$

$$f(x) = A_1 e^{j\phi_1} \quad -2L < x < -L$$

$$= A_2 e^{j\phi_2} \quad -L < x < 0$$

$$= A_3 e^{j\phi_3} \quad 0 < x < L$$

$$= A_4 e^{j\phi_4} \quad L < x < 2L$$

The closed form solution of this integral is programmed directly in terms of the quadrature detector output signals. All calibration constants are programmed in terms of their resultant sums using trig identities so that no arc tangent calculations are ever required. The transformation from the reference plane to the array aperture is done with identities also so that the calculations are as efficient as possible.

The program is stored on disk on the DAS-1800, which is service-interrupted when data is available for transfer from the drum to the 1800. A teletype is used to issue software commands to the PDP-8/1 controller and a storage scope is used to display graphic output while hard copy output is spooled for the line printer.

All transferred data is archived on a removable disk pack so that exhaustive processing may be completed at convenient times.

Since the quadrature detectors are linear, only one gain constant is required to scale them. However, the square law detectors are modeled by a second order polynomial which relates output power in kilowatts to input voltage.

A highly interactive, Fletcher-Powell optimization code is written for fitting the polynomial to the calibration data for each square law detector.

Table 1 shows the result of a curve fitting program run. The errors are in Power (kW). The maximum deviation between the polynomial and data is +0.097 dB at -18 dBm input power.

Table 1

SQUARE LAW DETECTOR
SAMPLE CURVE FIT DATA

X(1) = 2.3831077066D-02 G(1) =-3.2875748940D-05
X(2) = 9.8250483889D+01 G(2) = 2.7265826765D-07
X(3) =-1.1721608726D+01 G(3) = 2.6067883980D-07

W	Z	Power	F(X,W)	Error
0.00319	-40.00	0.331	0.337	0.018
0.00515	-38.00	0.525	0.530	0.008
0.00814	-36.00	0.832	0.823	-0.010
0.01300	-34.00	1.318	1.299	-0.014
0.02060	-32.00	2.089	2.043	-0.022
0.03340	-30.00	3.311	3.292	-0.005
0.05310	-28.00	5.248	5.208	-0.007
0.08420	-26.00	8.318	8.213	-0.012
0.13530	-24.00	13.183	13.108	-0.006
0.21760	-22.00	20.893	20.848	-0.002
0.35780	-20.00	33.113	33.677	0.017
0.58700	-18.00	52.481	53.658	0.022
0.96800	-16.00	83.176	84.147	0.011
1.63300	-14.00	131.826	129.209	-0.019

Acknowledgements

The author expresses thanks and a
to A. W. Weissenburger, A. J. Greenber
Thompson, G. and K. Hovey who, with th
have developed the computer hardware a
and to R. W. Motley who did the fourie
This work was supported by U. S. Ener
and Development Administration under
E(11-1)-3073.

References

[1] S. Bernabei, M. A. Heald, W. M.
F. J. Paoloni, "Penetration of S
into a Dense Plasma Using a Phas
Array,". Princeton Plasma Physi
Report MATT-1112, February 1975.

[2] van der Ziel, Solid State Physic
Prentice Hall, Inc., New Jersey,

[3] A. M. Cowley, H. O. Sorenson, "C
Comparison of Solid-State Microw
tors", IEEE Transactions on Micr
and Techniques, Vol. MTT-14, No.
602, December 1966.

[4] J. D. Dyson, "The Measurement of
and Microwave Frequencies", IEEE
on Microwave Theory and Techniqu
MTT-14, No. 19, p. 410-423, Sept

[5] R. A. Sparks, "A Phase Measuring
Short RF Pulses", IRE Transactio
Instrumentation, Vol. I-11, p. 2
December 1962.

[6] Morse and Feshbach, Methods of
Physics, McGraw-Hill, New York,

Figures

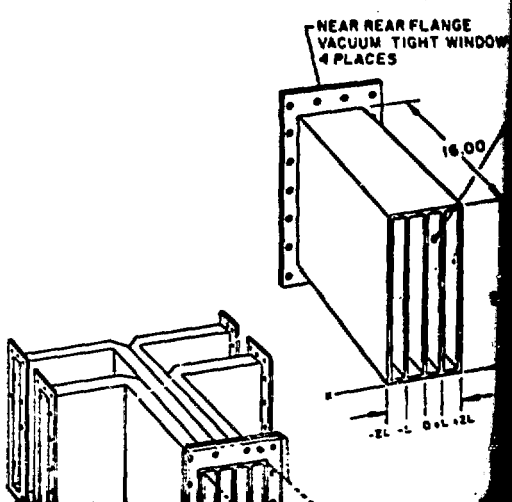

Acknowledgements

The author expresses thanks and appreciation to A. W. Weissenburger, A. J. Greenberger, P. A. Thompson, G. and K. Hovey who, with their associates have developed the computer hardware and software, and to R. W. Motley who did the fourier analysis. This work was supported by U. S. Energy Research and Development Administration under contract E(11-1)-3073.

References

[1] S. Bernabei, M. A. Heald, W. M. Hooke and F. J. Paoloni, "Penetration of Slow Waves into a Dense Plasma Using a Phased Waveguide Array,". Princeton Plasma Physics Laboratory, Report MATT-1112, February 1975.

[2] van der Ziel, Solid State Physical Electronics. Prentice Hall, Inc., New Jersey, 1968, p. 331.

[3] A. M. Cowley, H. O. Sorenson, "Quantitive Comparison of Solid-State Microwave Detectors", IEEE Transactions on Microwave Theory and Techniques, Vol. MTT-14, No. 12, p. 588-602, December 1966.

[4] J. D. Dyson, "The Measurement of Phase at UHF and Microwave Frequencies", IEEE Transactions on Microwave Theory and Techniques, Vol. MTT-14, No. 19, p. 410-423, September 1966.

[5] R. A. Sparks, "A Phase Measuring System for Short RF Pulses", IRE Transactions on Instrumentation, Vol. I-11, p. 298-302, December 1962.

[6] Morse and Feshbach, Methods of Theoretical Physics, McGraw-Hill, New York, 1953, p. 453.

Figures

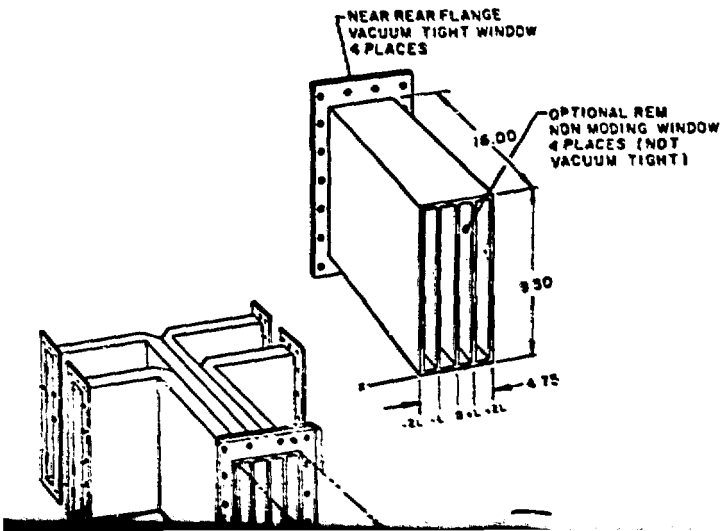

able for transfer from the drum to the 1800. A teletype is used to issue software commands to the PDP-8/I controller and a storage scope is used to display graphic output while hard copy output is spooled for the line printer.

All transferred data is archived on a removable disk pack so that exhaustive processing may be completed at convenient times.

Since the quadrature detectors are linear, only one gain constant is required to scale them. However, the square law detectors are modeled by a second order polynomial which relates output power in kilowatts to input voltage.

A highly interactive, Fletcher-Powell optimization code is written for fitting the polynomial to the calibration data for each square law detector.

Table 1 shows the result of a curve fitting program run. The errors are in Power (kW). The maximum deviation between the polynomial and data is +0.097 dB at -18 dBm input power.

Table 1

SQUARE LAW DETECTOR
SAMPLE CURVE FIT DATA

X(1) = 2.3831077066D-02 G(1) =-3.2875748940D-05
X(2) = 9.8250483889D+01 G(2) = 2.7265826765D-07
X(3) =-1.1721608726D+01 G(3) = 2.6067883980D-07

W	Z	Power	F(X,W)	Error
0.00319	-40.00	0.331	0.337	0.018
0.00515	-38.00	0.525	0.530	0.008
0.00814	-36.00	0.832	0.823	-0.010
0.01300	-34.00	1.318	1.299	-0.014
0.02060	-32.00	2.089	2.043	-0.022
0.03340	-30.00	3.311	3.292	-0.005
0.05310	-28.00	5.248	5.208	-0.007
0.08420	-26.00	8.318	8.213	-0.012
0.13530	-24.00	13.183	13.108	-0.006
0.21760	-22.00	20.893	20.848	-0.002
0.35780	-20.00	33.113	33.677	0.017
0.58700	-18.00	52.481	53.658	0.022
0.96800	-16.00	83.176	84.147	0.011
1.63300	-14.00	131.826	129.209	-0.019

Cost = 2.44991603100-02
W = output voltage; Z = input power (dBm);
Power = equivalent system power input (kW)

$$\text{Error} = \frac{F(X,W)}{\text{Power}} - 1$$

$$\text{Cost} = \sqrt[10]{\sum (\text{Error})^{10}}$$

$$F(X,W) = X(1)+X(2)W+X(3)W^2$$

[1] S. Bernabei, M. A. Heald, W. M. Hoo
F. J. Paoloni, "Penetration of Slow
into a Dense Plasma Using a Phased
Array,". Princeton Plasma Physics
Report MATT-1112, February 1975.

[2] van der Ziel, Solid State Physical
Prentice Hall, Inc., New Jersey, 19

[3] A. M. Cowley, H. O. Sorenson, "Quant
Comparison of Solid-State Microwave
tors", IEEE Transactions on Microwa
and Techniques, Vol. MTT-14, No. 12,
602, December 1966.

[4] J. D. Dyson, "The Measurement of Ph
and Microwave Frequencies", IEEE Tr
on Microwave Theory and Techniques,
MTT-14, No. 19, p. 410-423, Septemb

[5] R. A. Sparks, "A Phase Measuring Sy
Short RF Pulses", IRE Transactions
Instrumentation, Vol. I-11, p. 298-
December 1962.

[6] Morse and Feshbach, Methods of Theo
Physics, McGraw-Hill, New York, 195

Figures

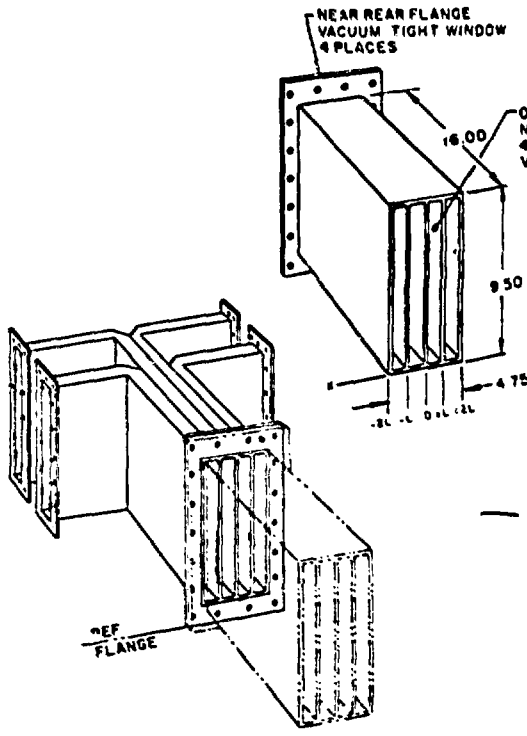

Fig. 1 - Feed Assembly

3

[1] S. Bernabei, M. A. Heald, W. M. Hooke and F. J. Paoloni, "Penetration of Slow Waves into a Dense Plasma Using a Phased Waveguide Array,". Princeton Plasma Physics Laboratory, Report MATT-1112, February 1975.

[2] van der Ziel, Solid State Physical Electronics. Prentice Hall, Inc., New Jersey, 1968, p. 331.

[3] A. M. Cowley, H. O. Sorenson, "Quantitive Comparison of Solid-State Microwave Detectors", IEEE Transactions on Microwave Theory and Techniques, Vol. MTT-14, No. 12, p. 588-602, December 1966.

[4] J. D. Dyson, "The Measurement of Phase at UHF and Microwave Frequencies", IEEE Transactions on Microwave Theory and Techniques, Vol. MTT-14, No. 19, p. 410-423, September 1966.

[5] R. A. Sparks, "A Phase Measuring System for Short RF Pulses", IRE Transactions on Instrumentation, Vol. I-11, p. 298-302, December 1962.

[6] Morse and Feshbach, Methods of Theoretical Physics, McGraw-Hill, New York, 1953, p. 453.

Figures

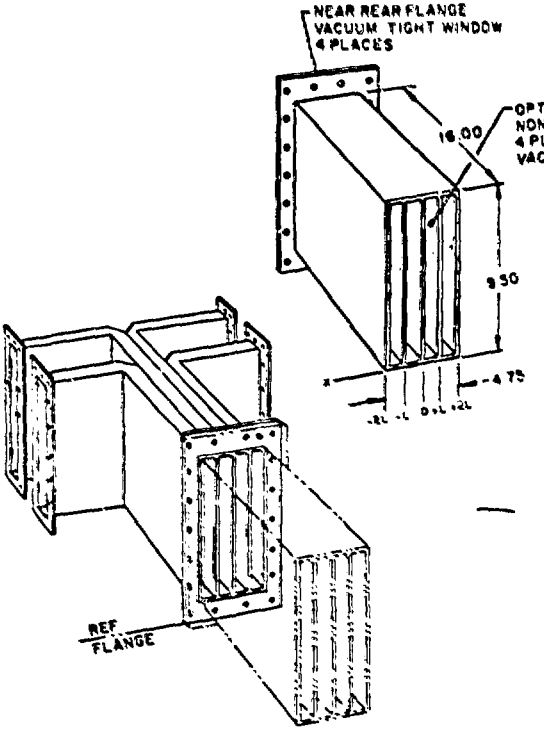

Fig. 1 - Feed Assembly

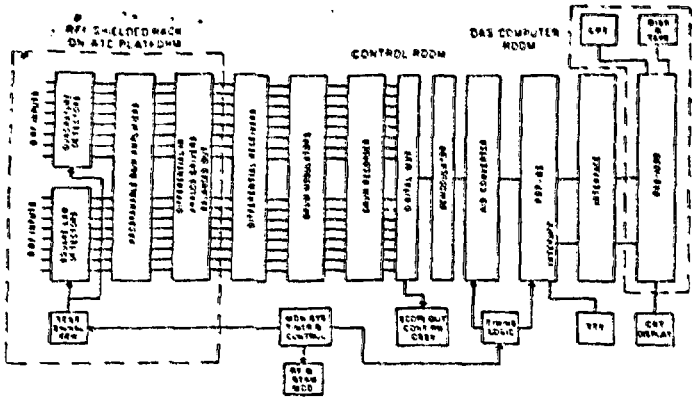

Fig. 2 - Data Processing System

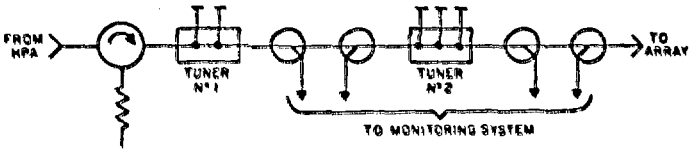

Fig. 3 - Transmission System

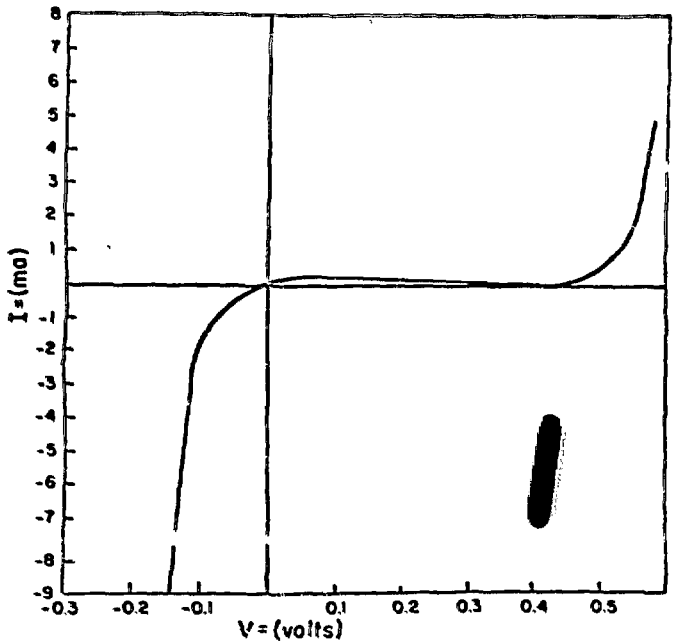

Fig. 4 - BD-3 V-I Curve

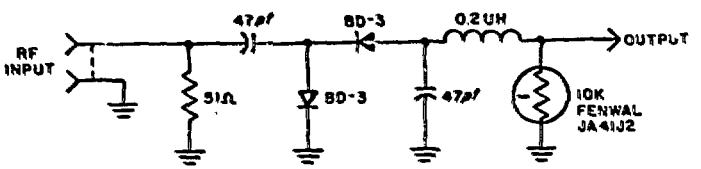

Fig. 5 - Square Law Detector Schematic

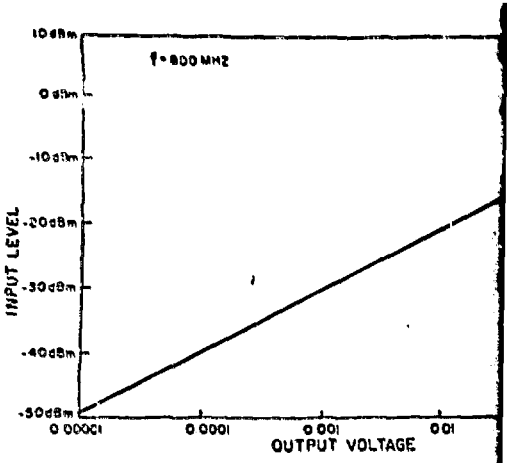

Fig. 7 - Typical Square Law Detector

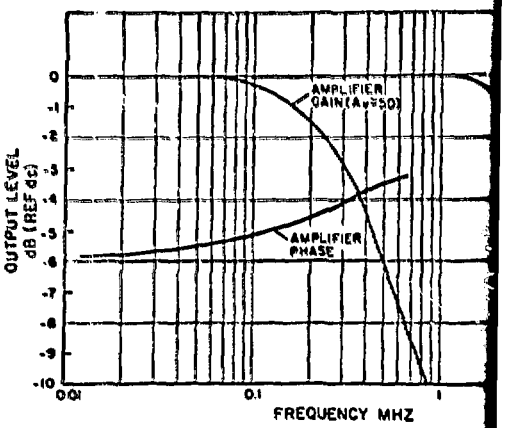

Fig. 8 - Detector and Amplifier

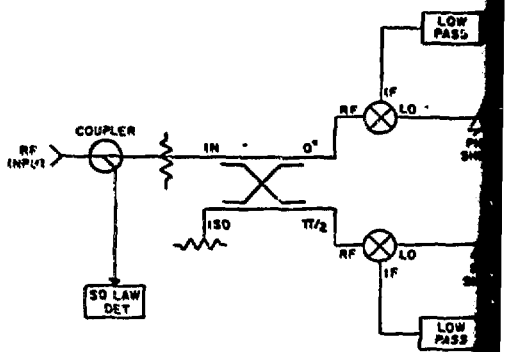

Fig. 9 - Quadrature Detector B

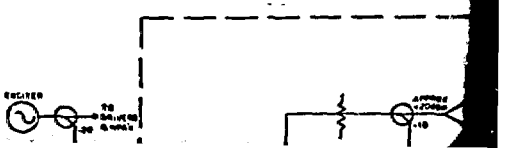

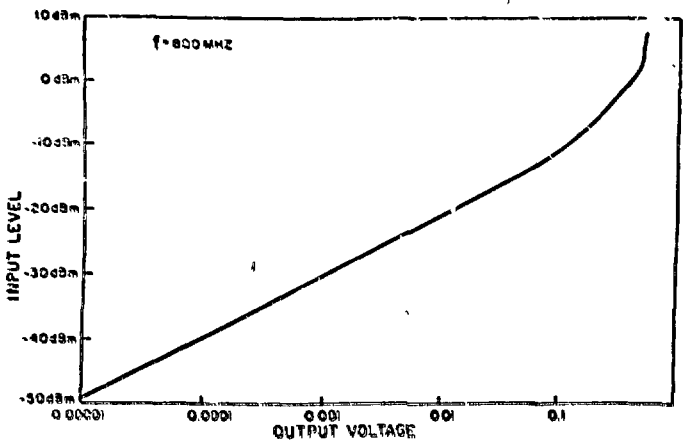

Fig. 7 - Typical Square Law Detector Performance

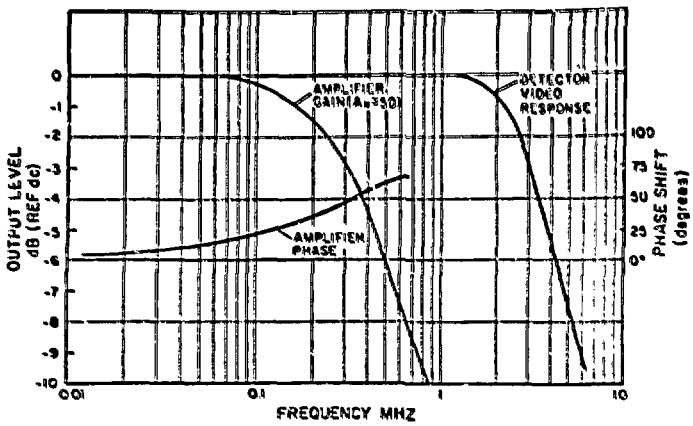

Fig. 8 - Detector and Amplifier Response

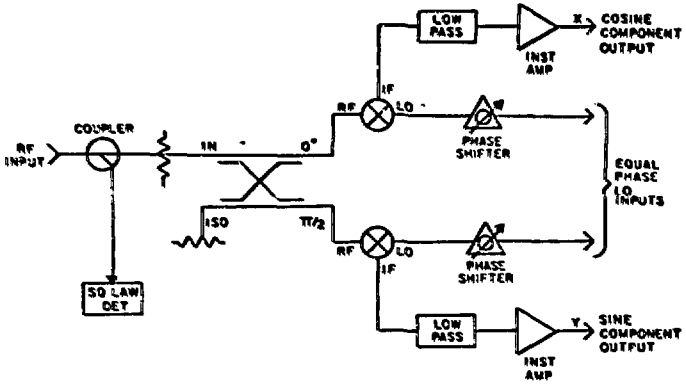

Fig. 9 - Quadrature Detector Block Diagram

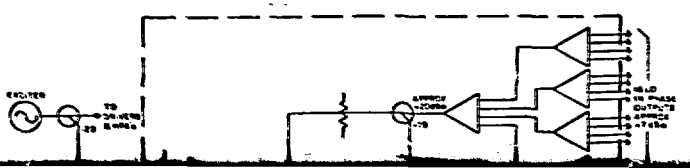

Fig. 2 - Data Processing System

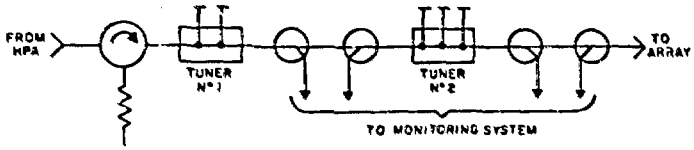

Fig. 3 - Transmission System

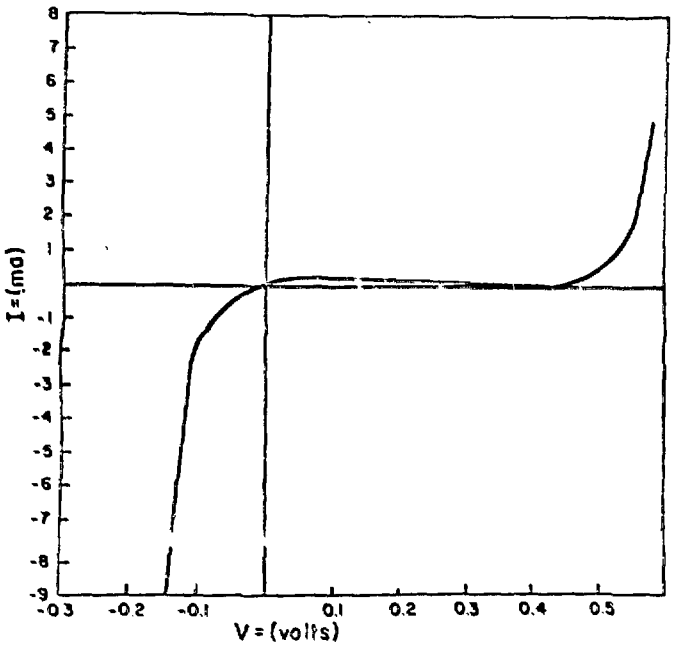

Fig. 4 - BD-3 V-I Curve

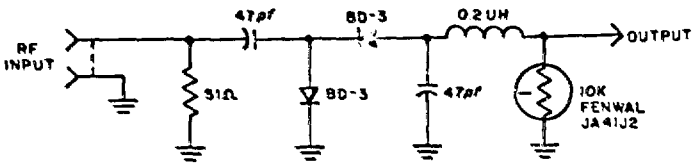

Fig. 5 - Square Law Detector Schematic

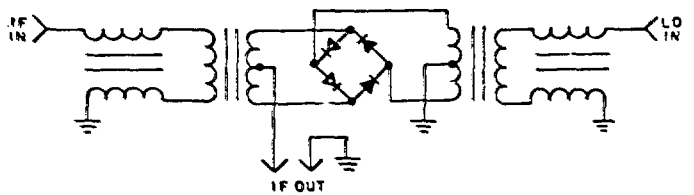

Fig. 6 - Double Balanced Mixer Schematic

Fig. 7 - Typical Square Law Detector Per

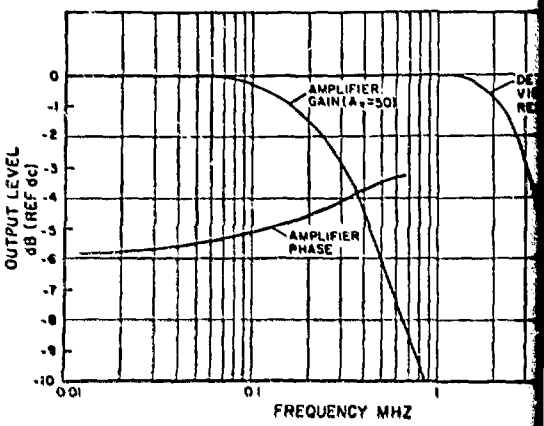

Fig. 8 - Detector and Amplifier Res

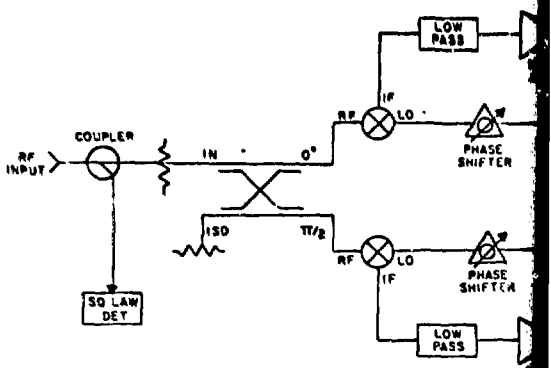

Fig. 9 - Quadrature Detector Block

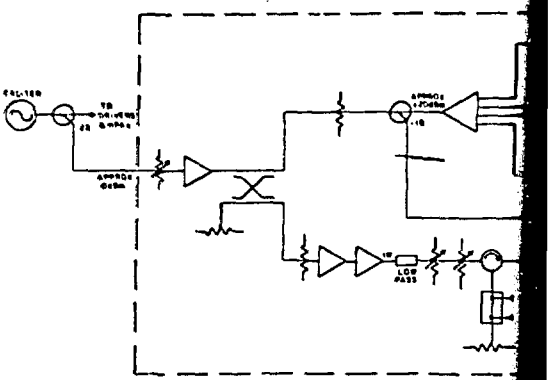

Fig. 10 - Power Splitter Block D

3

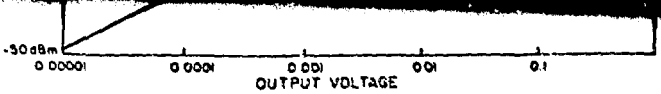

Fig. 7 - Typical Square Law Detector Performance

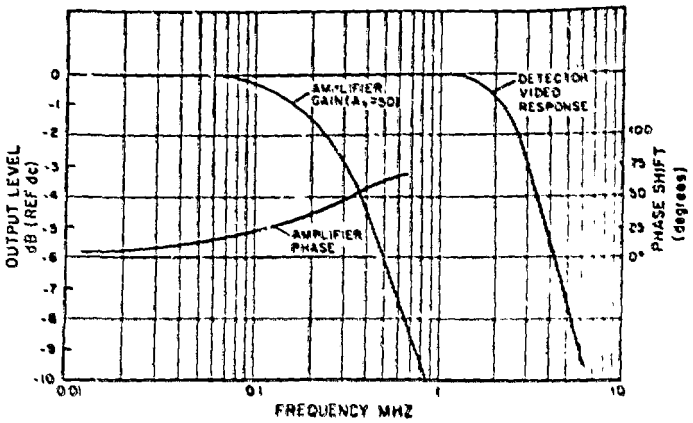

Fig. 8 - Detector and Amplifier Response

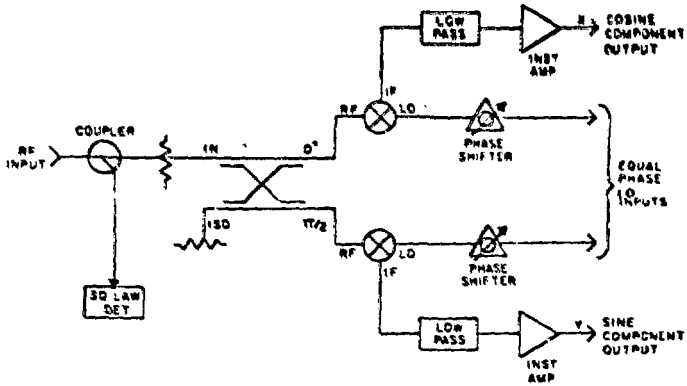

Fig. 9 - Quadrature Detector Block Diagram

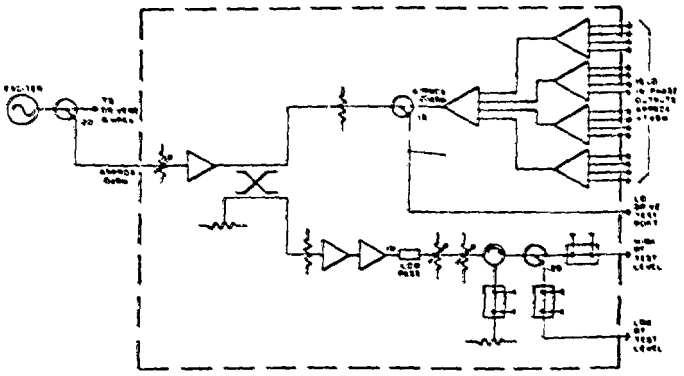

Fig. 10 - Power Splitter Block Diagram

4